https://erjm.journals.ekb.eg
ISSN: 1110-1180

DOI: ---------

**ERJ**
**Engineering Research Journal**
**Faculty of Engineering**
**Menoufia University**

# Numerical Analysis of Turbulent Flow in a 3-D Horizontal Finned Tube with Uniform Heat Flux

**Omar Hamdy Salem, Ahmed Hegazy, Khaled Yousef***

*Department of Mechanical Power Engineering, Menoufia University, Shebin-Elkom, Egypt.*
**Corresponding author (ng_khalid@yahoo.com)*

**ABSTRACT**
The present paper presents a CFD study to determine the heat transfer and fluid flow characteristics of finless and internally continuous finned tubes at different flow conditions. The numerical investigation is executed by solving the conservation equations of mass, momentum, and energy along with two equation-based realizable $K-\varepsilon$ model with enhanced wall treatment for thermal and hydrodynamic effects to determine the Nusselt number and the friction factor for finned and finless tubes. The proposed CFD model has been validated with the results available in the literature of previous experimental works. The numerical results showed a good agreement with these experimental ones. It has been found from the present study that increasing fin height and row number leads to a significant enhancement in thermal performance but results in high pumping power for fluid through finned tubes. Also, fin height has more effect on the thermal performance of the finned tube compared to the number of rows. Fin thickness has insignificant effect on thermal performance. Also, a finned tube enhances heat transfer and pressure drop compared to a finless one. In some cases, the heat transfer coefficient is enhanced 9 times in value compared to the finless one. But also, the friction coefficient rises to 2 times in value in the same case. Generally, a finned tube can be integrated with a heat exchanger to become more reliable and efficient.

***Keywords:*** *Friction factor, Nusselt number, Finless tube, Finned tube, Heat transfer applications.*

## 1. Introduction

Internally continuous finned tubes have been widely used in numerous technical applications to improve heat transfer characteristics. A further enhancement of heat transfer in heat exchangers is economically very beneficial as it is used in many fields of engineering; e.g. power plants, chemical processes, petroleum industries, etc. The current study presents a 3-D numerical analysis of convective heat transfer for internally finned tubes. Also, the heat transfer coefficient and pressure drop within these tubes will be assessed. Ahsan [1] studied numerically the fully turbulent flow in a pipe at a higher Reynolds number. He proved that the $k-\varepsilon$ model with enhanced wall treatment is computationally cheap and a good choice to predict thermal and hydrodynamic performance inside tubes. Bolukbasi et al. [2] discussed the turbulent flow inside a 2-D tube with uniform heat flux. They found that the Nusselt number increases and the friction factor decreases with the Reynolds number. Everts et al. [3] investigated experimentally the heat transfer characteristics of developing flow in transitional flow regimes with variable Reynolds number. They found the transition end delays with increasing the distance along the whole tube length and occurred earlier with increasing heat flux. Meyer et al. [4] conducted heat transfer and pressure drop experiments in the quasi-turbulent and turbulent flow regimes to develop an accurate heat transfer correlation that can be used as a single correlation that is valid for all flow regimes. They succeeded to correlate a single Nusselt number correlation that is valid for laminar, transitional, quasi-turbulent, and turbulent flow. Belhocine et al. [5] made a numerical study to simulate thermal characteristics inside thermally developing turbulent flow. It has been found that wall temperature is higher with magnifying the Reynolds number and the local Nusselt number increases with the Reynolds number. Gbadebo et al. [6] carried out experiments to get a correlation for the average Nusselt number for pulsating turbulent flow. They proved that flowrate was periodically varied at frequencies ranging from 1 Hz to 13 Hz while the average Reynolds number varied from 6400 to 42000. Sahin et al. [7] conducted an experimental study on heat transfer and pressure drop for flow inside pipes. They found that the Nusselt number increases, and the friction factor decreases with the Reynolds number. They compared numerical values with the correlations of Pethukov [27] and Blasius with small errors. Huq et al. [8] conducted an experimental study on measurements of heat transfer in an internally finned tube. This study led to inferring that at a higher Reynolds number, the wall temperature is low. Also, it was concluded that, in the case of a finned tube, less heat is taken away by the working fluid and the thermal entrance length compared to finless tube one is less. Patankar et al. [9] studied analytically the turbulent flow and heat transfer inside the finned tube using the mixing length method. They proved that by increasing row number, the total flow rate through the inter-face spaces decreases, and the local fin heat transfer coefficient varied significantly along with fin height. Kim et al. [10] made an analytical prediction for the friction factor and heat transfer for turbulent flow inside internally finned tubes. They proved that the wall shear stress is maximum at the fin tip and decreases with the fin surface. Also, the fin surface temperature is assumed to vary linearly from the fin tip to the fin base. Carnavos [11,12] conducted experiments to assess the heat transfer performance of internally finned tubes in a turbulent flow. It has been proved that finned tubes are capable of increasing heat exchanger capacity. Mohapatra et al. [13] made a numerical investigation to determine the friction factor and the Nusselt number of an internally finned tube. It has been found that heat transfer to fluid is maximum up to a certain height of the fin after that the flow path is clogged and the turbulent mixing cannot occur properly and the Nusselt number is continuously decreasing along the tube length. Islam et al. [14] studied experimentally the thermal performance for T-shaped finned tubes having the Reynolds numbers ranging from 20,000 to 50,000. They found that friction factor is 5 times higher and the heat transfer coefficient is 2 times higher than those for smooth tube for the same flow conditions. Nandakumar et al. [15] studied numerically the fully developed viscous flow in internally finned tubes. They proved that moving fluid near the wall is strongly dependent on the Reynolds number and the moving flow in the central core is faster, which is independent of the angular direction. Soliman et al. [16] analytically studied the fully developed laminar flow in longitudinal internally finned tubes. This work proved that velocity gradient in both the radial and angular directions becomes steeper near the solid boundaries and also there's an increase in pressure drop accompanying the increase in half the angle subtended by one fin. El-Sayed et al. [17,18] studied experimentally pressure distribution for turbulent flow inside a circular finned tube. They proved that the Nusselt number and the friction factor for a finned tube is higher than finless tube values. Fabbrii [19] studied numerically the performance of internally finned tubes under laminar flow conditions. He proved that the heat flux dissipated per unit of surface is inversely proportional to the tube radius. Alam et al. [20] worked on a numerical study to assess the heat transfer effectiveness of circular tubes with internal longitudinal fins having tapered lateral profiles. They proved that water is a more effective coolant compared to engine oil and this is due to the high thermal conductivity of water. Zeiton and Hegazy [21] studied numerically heat transfer for laminar flow in internally finned pipes with different fin heights and uniform wall temperature. They revealed that the height of one fin gets shorter, its contribution to heat transfer is reduced while the contribution of the longer fin is enhanced. Also, the coefficient of friction grows steeply as the number of fins is increased. Kim et al. [22] studied numerically the thermal performance of internally finned tubes with variable fin thickness. He proved that the smaller the number of fins, the lower is the capacitive resistance and finned tube with variable fin thickness. Kim et al. [23] discussed the fluid flow and heat transfer characteristics in a helically-finned tube. They proved that the performance of the helically-finned tube based on the area and volume goodness factor is much worse than in the case of a straight circular tube. He also proved that the turbulence intensity rises with increasing the fin height and also magnifies with increasing the Reynolds number. Khanmohammadi et al. [24] made a numerical study on the heat transfer and fluid flow characteristics inside a tube with internal star fins. They proved that adding fins increases the heat transfer surfaces and augments the heat transfer rate. Also, the temperature of fluid increases by adding more fins as the temperature of the tube wall is decreased.

The objective of this numerical study is to determine the thermal and the hydrodynamic characteristics of tubes equipped by internal straight fins. And also constructing a comparison between these tubes and tubes with no fins. fin height, rows number, thickness, Reynolds number and other parameters are changed during the study to reveal their effects on performance of finned tubes.

## 2. Mathematical formulation

The present CFD simulation is a 3-D steady forced turbulent convection flow of pure water in a finned and finless tube. Figure (1) shows the domain of this simulation. The tube has a diameter of 5.6 cm and thickness of 0.5 cm with an inlet insulated section with 50 cm length to ensure that the flow enters the test section as nearly fully developed and 100 cm length for the rest. For the finned tube, row number changes from 1 to 4 and fin height ranges from 1 cm to 2 cm. Both smooth and finned tubes are numerically studied with different Reynolds numbers. The flow is assumed to be incompressible fluid with constant thermo-physical properties. Saturated water tables are used to get the properties of water.

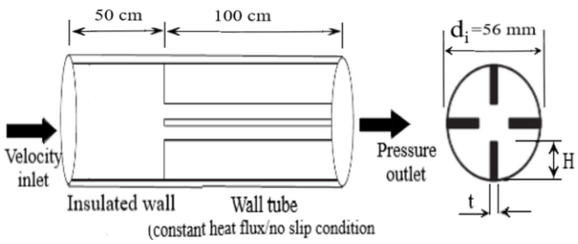


Figure (1)- Considered finned tube in the present CFD simulation

**2.1. Governing equations**

Continuity:

$$\frac{\partial}{\partial x_i}(\rho\, v_i) = 0 \qquad (1)$$

Momentum:

$$\frac{\partial}{\partial x_j}\left(\rho\, v_i\, v_j\right) = -\frac{\partial p}{\partial x_i} + \frac{\partial}{\partial x_j}\left[\mu\left(\frac{\partial v_i}{\partial x_j} + \frac{\partial v_j}{\partial x_i}\right) - \rho\, \overline{v_i^{`}\, v_j^{`}}\right] \qquad (2)$$

Where

$$-\overline{v_i^{`}\, v_j^{`}} = 2\frac{\mu_t}{\rho} S_{ij} \text{ and } S_{ij} = \frac{1}{2}\left(\frac{\partial v_i}{\partial x_j} + \frac{\partial v_j}{\partial x_i}\right) \qquad (3)$$

Energy:

$$\frac{\partial}{\partial x_i}\left(\rho\, C_p v_i\, T\right) = -\frac{\partial}{\partial x_i}\left[\left(-k\frac{\partial T}{\partial x_i}\right) + \rho\, C_p\, \overline{v_i^{`}\, T^{`}}\right] \qquad (4)$$

Conduction:

$$\frac{\partial}{\partial x_i}\left(k\frac{\partial T}{\partial x_i}\right) = 0 \qquad (5)$$

The realizable $K-\varepsilon$ model is used to simulate the turbulence in the present simulation. Also, enhanced wall treatment with pressure and thermal effect is used along with the realizable $K-\varepsilon$ model to solve the boundary layer near the walls.

**2.2. Boundary conditions**

Uniform axial velocity is considered at the tube inlet, which corresponds to mass flowrate ranging from 0.2351 to 0.5486 kg/s while the temperature changes from 15 to 35 $^oC$. At the tube exit, outlet static pressure, which equals zero gage pressure, is utilized. The no-slip boundary condition is used on the whole wall of the pipe. Uniform heat flux ranging from 1000 W to 5000 W is imposed on the last 100 cm heated wall and zero heat flux at the first 50 cm for the insulated wall is used.

**2.3. Computation of the most important heat transfer and fluid flow parameters**

The most important parameters used in the present computation are shown below. These parameters are utilized to describe the flow field and heat transfer characteristics.

1-bulk temperature: $T_b = \frac{T_i + T_o}{2}$
Where water properties are calculated at $T_b$

2-Internal surface area: $A_s = \pi\, d_i\, L$

3-Finned Cross section area: $A_c = (\pi/4)\; d_i^2 - N\, H\, t$

4-Inlet Cross section area: $A_i = (\pi/4)\; d_i^2$

5-Hydraulic diameter: $d_h = [4\, A_c]/\,[\pi\, d_i + 2\, N\, H]$

6-Mass flowrate: $\dot{m} = \rho\, A_i\, V_i$

7-Average velocity through finned section: $V_f = \frac{\dot{m}}{\rho\, A_c}$

8-Reynolds number based on $d_i$ : $Re = \frac{\rho\, V_f\, d_i}{\mu}$

9-Reynolds number based on $d_h$: $Re_h = \frac{\rho\, V_f\, d_h}{\mu}$

10-Local friction factor based on $d_i$ : $f = \frac{2\, \Delta p\, d_i}{\rho\, V_f^2\, x}$

11-Local friction factor based on $d_h$: $f_h = \frac{2\, \Delta p\, d_h}{\rho\, V_f^2\, x}$
Where $\Delta p$ measured across x distance.

12-Heat flux applied on tube wall: $q = \frac{\dot{m}\, C_p\, (T_o - T_i)}{A_s}$

13-Mean temperature along tube: $T_m = T_i + \frac{q\, \pi\, d_i}{\dot{m}\, C_p}\, x$

14-Local heat transfer coefficient: $h = \frac{q}{(T_w - T_m)}$

15-Local Nusselt number based on $d_i$: $Nu = \frac{h\, d_i}{k}$

16-Local Nusselt number based on $d_h$: $Nu_h = \frac{h\, d_h}{k}$

**3. Numerical solution procedure**

Steady three-dimensional equations of mass, momentum, energy and turbulence modeling have been solved by the commercial solver Fluent 19. A second-order upwind scheme (for convective variables) was considered for momentum as well as for the turbulent discretized equations. The mesh near the tube wall and the fin surface area was refined till $y^+$ (wall distance which effects turbulence) near the wall is equal or less than unity. This will ensure that the boundary layer will be solved precisely, especially the viscous sublayer near the wall and this gives a good opportunity to capture the flow fields inside the tube and near the walls. SIMPLE algorithm with the second order scheme for pressure has been used. The realizable $K - \varepsilon$ model is utilized to simulate the turbulence in the present simulation since this model is believed to provide superior performance for complex flows [1,13,25,26]. A convergence of the discretized equations is believed to have been achieved when the whole field residuals for all the variables fell below $10^{-3}$ except for the energy equation residual which is set to $10^{-6}$.

**4. Grid sensitivity test**

A grid sensitivity test is performed for the cases of finless and finned tubes. Different grid numbers are used from 900000 cells to 6 million cells. The exit mean temperature is calculated and nearly three and half million cells for the finless tube and nearly 3800000 cells for the finned tube are chosen for good results. Figure (2) is the cross-sectional view of both finless and internally finned tubes. Figure (3) shows the mesh independence study for finless and finned tubes.

**5. Validation of the Computational Model**

The results are validated by using an inlet temperature $T_i$ = 20 °C with a mass flowrate ranging from 0.2351 to 0.5486 kg/s. In order to validate the computational model, the numerical results were compared with the results of the well-known correlations for fully developed flow inside tubes. Nusselt number computed with the present simulation for developed turbulent flow were compared with the equation given by Petukhov [27]:

$$\mathrm{Nu} = \frac{\mathrm{Re} * \mathrm{Pr} * \frac{f}{2}}{c + 12.7 * \left(\frac{f}{2}\right)^{0.5} * \left(\mathrm{Pr}^{\frac{2}{3}} - 1\right)}$$

$$\text{where}, C = 1.07 + \frac{900}{\mathrm{Re}} - \frac{0.63}{1 + 10 * \mathrm{Pr}} ,$$

$$\text{and} \quad f = (0.79 \ln(\mathrm{Re}) - 1.64)^{-2}$$

Figure (4) shows the comparison of the Nusselt number from the Petukhov equation and the computed values from the present CFD study for water. The maximum deviation of the computed Nusselt number from the equation given by Petukhov is 2.2 %. The friction factor values were compared with the friction factor given by the Petukhov equation [27]:

$$f = (0.79 \ln(\mathrm{Re}) - 1.64)^{-2}$$

Figure (5) displays the comparison of the friction factor from the Petukhov equation versus the computed values using this numerical study, which shows a good agreement with the experimental results [27].

**6. Results and discussion**

**6.1. Finless tube results**

**6.1.1. Reynolds number effect on the Nusselt number**

Figure (6) shows the effect of Reynolds number on the Nusselt number for different inlet temperatures. It's obvious from the figure that increasing the Reynolds number leads to a rise in the Nusselt number. Augmenting the Reynolds number means raising the inertia force, i.e. the mean velocity, which leads to an augmentation in the bulk motion of the fluid. This means enhancing the heat transfer by convection and hence rising the Nusselt number. Also, it's obvious from the same figure, as temperature rises, the Nusselt number grows. An increase in the temperature means decreasing Prandtl number ($\mathrm{Pr} = \frac{\upsilon}{\alpha}$), and hence it leads to an augmentation in thermal diffusivity and thermal boundary layer thickness. As a result, the heat transfer rate and the Nusselt number recede.

**6.1.2. Heat flux effect on the Nusselt number**

It is obvious that with the constant properties of the fluid, there is no heat flux effect on the Nusselt number. When heat flux augments, wall temperature and mean fluid temperature at every section of the tube grows and the temperature difference at any section remains constant, and hence the Nusselt number doesn't change. In table (2) the mean temperature of the fluid and the wall temperature of the tube as well as the Nusselt number are listed as a function of the distance for heat flux ranging from 1000 to 5000 W. Table (2) shows that the Nusselt number remains constant with heat flux.

**6.1.3. Reynolds number effect on the friction factor**

It is Shown from figure (7), which depicts the effect of the Reynolds number on the friction factor that as the Reynolds number gets lower, friction factor

detracts due to an augmentation in the Reynolds number which
means higher inertia force (i.e. mean velocity) and higher bulk motion of the fluid. Furthermore, increasing the dynamic pressure results in detraction in viscous force and shear stress where friction factor formula is given by:

$$f = \frac{\tau_w}{0.5 * \rho * V_f^2} \text{ , dynamic pressure } = 0.5 * \rho * V_f^2$$

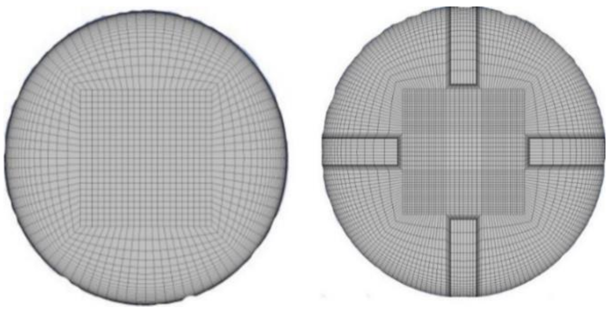

Figure (2)– Cross-sectional view of mesh for both finless and internally finned tubes

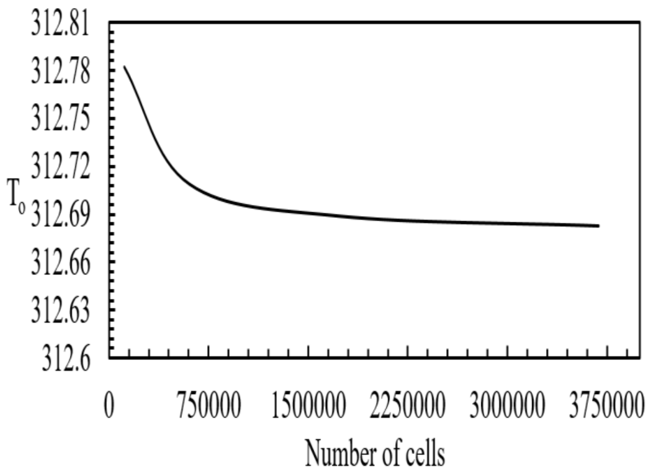


(3.a)- Mesh independence study for the finless tube

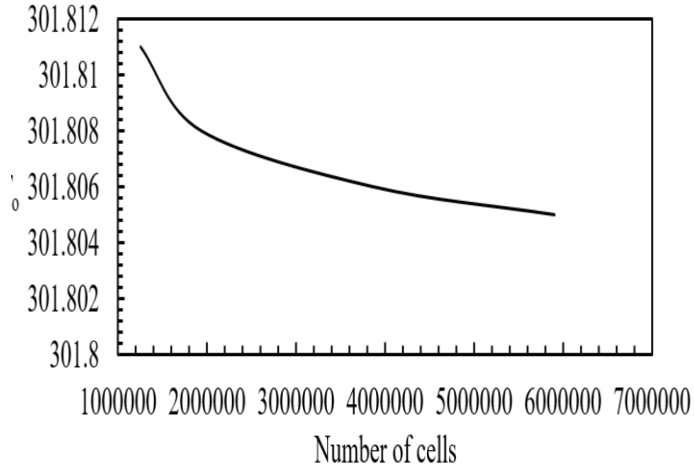


(3.b)- Mesh independence study for the finned tube

Figure (3)- Mesh independence study

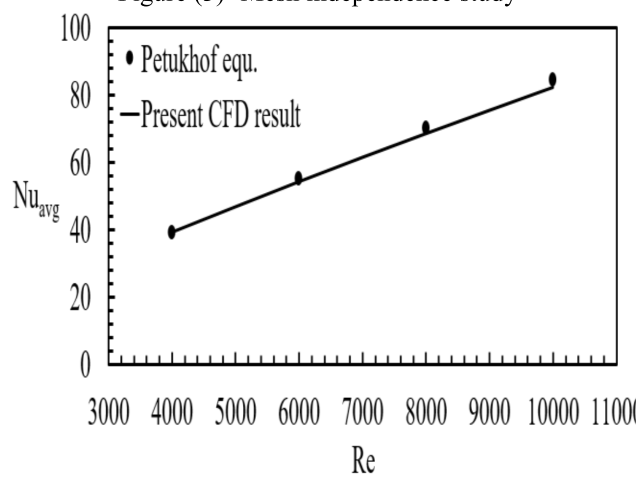


Figure (4)- Average Nu validation with the Petukhof equation

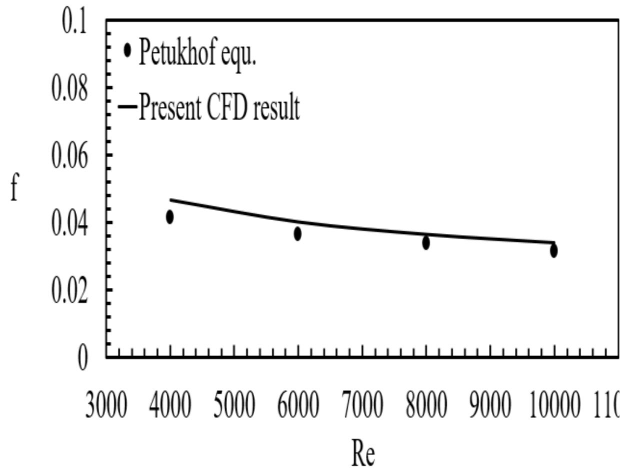


Figure (5)- Average f validation with the Petukhof equation

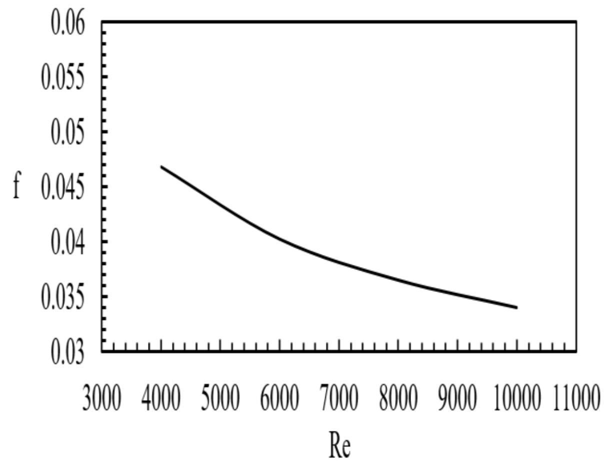


Figure (7)- Reynolds number effect on average friction factor for the finless tube

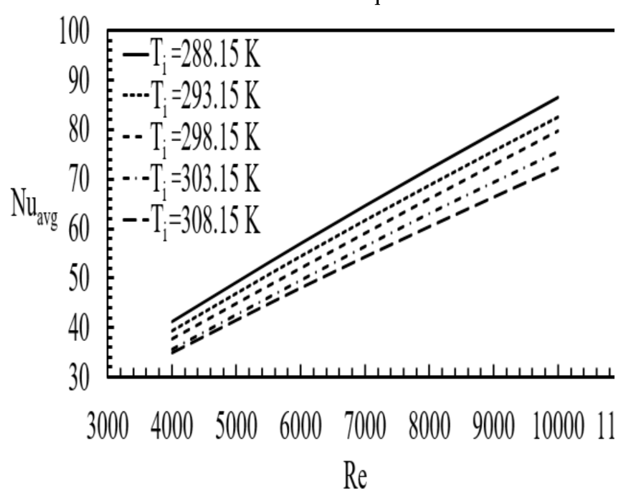


Figure (6)- Reynolds number effect on the average Nusselt number for the finless tube

Table (1) Nu no. values for different total heat input

| x (m) | Q = 1000 W | | Q = 5000 W | | Nu |
|---|---|---|---|---|---|
| | $T_m$ (k) | $T_w$ (k) | $T_m$ (k) | $T_w$ (k) | |
| 0.5 | 288.2 | 291.4 | 288.2 | 304.6 | 153.8 |
| 0.75 | 288.5 | 293.6 | 289.6 | 315.4 | 97.8 |
| 1 | 288.8 | 300.5 | 291.1 | 350 | 42.8 |
| 1.25 | 289.1 | 301.2 | 292.6 | 353.2 | 41.7 |

### 6.2. Finned tube results

#### 6.2.1. Fin height effect

For internally finned tubes, it is seen that the $H/d_i$ ratio plays a crucial role in heat transfer. Figures (8,9) illustrate how the $H/d_i$ ratio affects the Nusselt number and the friction factor in the finned tubes. It can be seen from figure (8) that, as the $H/d_i$ ratio of the fins rises from 0.1786 to 0.3571, the Nusselt number increases. When the fin height is larged, which means higher fin surface area and due to that more heat is transferred to fluid. Also, from figure (9) it is clear that as the $H/d_i$ ratio decreases the friction factor is minimized. When the fin height is magnified, higher fin surface area, hence more friction between the surface and fluid particles. This comparison was performed at a constant mass flowrate which equals 0.39188 kg/s.

#### 6.2.2. Effect of number of rows

For internally finned tubes, it is seen that the number of rows plays a crucial role in heat transfer. Figures (10,11) illustrate how row number affects the Nusselt number and the friction factor in the finned tubes. It can be seen from figure (10) that as the number of rows rises from 1 to 4, the Nusselt number soars. Also, from figure (11) as the number of rows raises, friction factor increases. This comparison is executed at a constant mass flow rate of 0.39188 kg/s. Both Nusselt number and friction factor climb with row number due to more surface area as discussed previously.

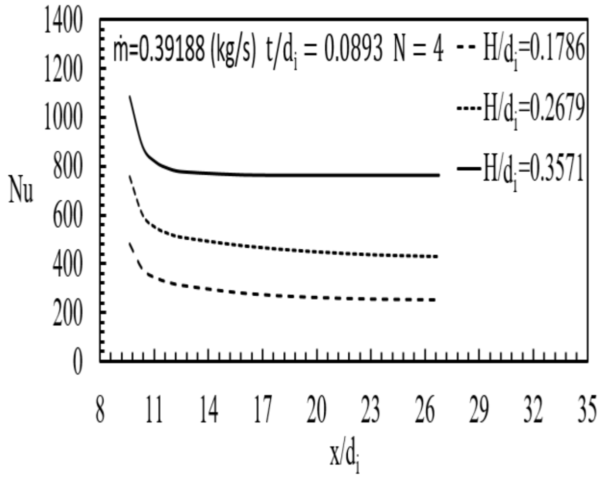

Figure (8)-Fin height effect on the local Nusselt number

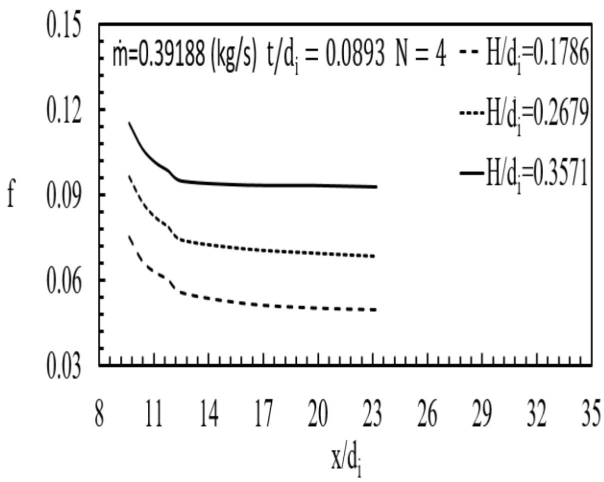

Figure (9)- Fin height effect on the local friction factor

### 6.2.3. Reynolds number effect

For flow inside tubes, it is seen that the Reynolds number plays a crucial role in heat transfer. It can be seen from figures (12,13), which reveal the effect of Reynolds number on the local Nusselt number and the friction factor, that, as the Reynolds number rises, the Nusselt number increases. An increase in the Reynolds number means a rise in inertia force which leads to more bulk motion of the fluid, more mixing between fluid layers, a thinner boundary layer, and less thermal resistance. And this means more heat transfer by convection and higher Nusselt number. Also, as the number of fins rises the friction factor decreases. Augmentation in the Reynolds number means higher inertia force and more bulk motion of the fluid, more mixing between fluid layers, increasing in dynamic pressure, detraction in shear stress, and friction factor.

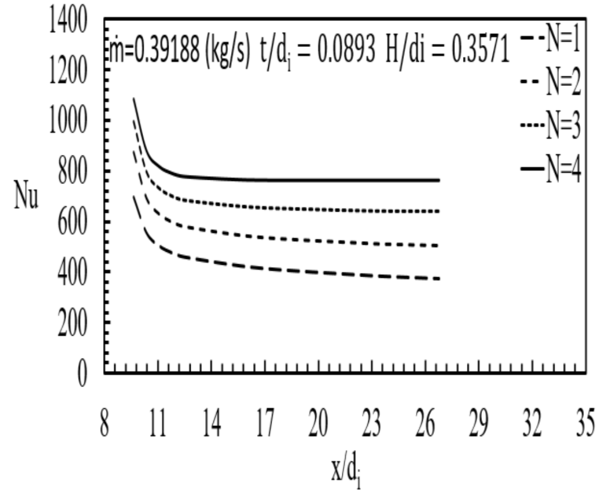

Figure (10)- Row number effect on the local Nusselt number

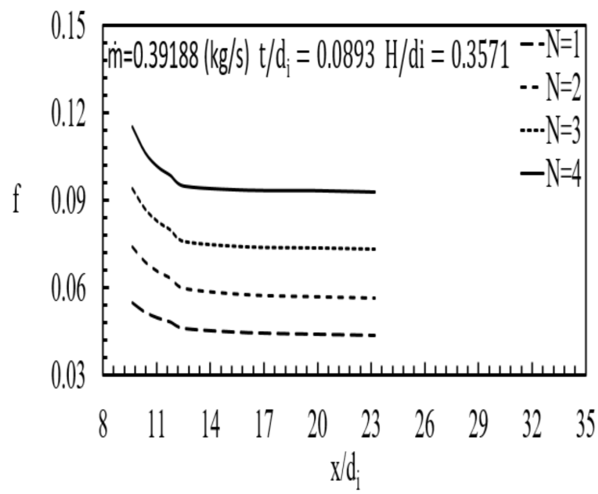

Figure (11)- Row number effect on the local friction factor

To assess the performance of finned tubes compared to finless ones, Figure (14) represents the average Nusslet number for the finned and finless tubes. This comparison is based on the same mass flowrate through finned and finless ones. From the figure, it is seen that the average Nusselt number for the finned tubes is higher compared to the tubes with no fins due to lower contact area between fluid and the tube surface for finless and also higher velocity in between finned sections which results in a higher heat transfer coefficient. Also, from figure (15) it is seen that, the average friction factor along the finned tube is higher for the finned tubes compared to the tubes with no fins. This is due to, as mentioned earlier, enhanced contact area between the fluid and the tube surface for finned and higher velocity in between the finned sections which results in higher friction factor.

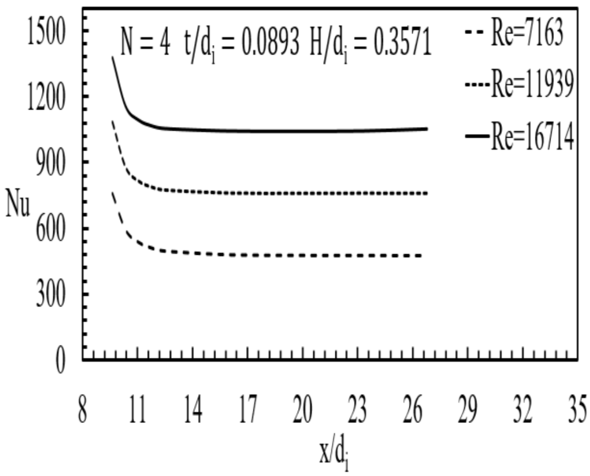


Figure (12)- Reynolds number effect on the local Nusselt number for the finned tube

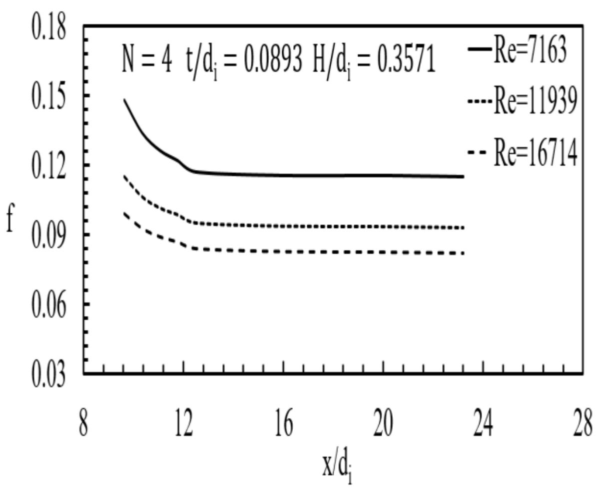


Figure (13)- Reynolds number effect on the local friction factor for the finned tube

**7. Study of the hydrodynamic and thermal CFD contours**

To illustrate the overall performance of the finned tubes, figure (16) shows that the hydrodynamic boundary layer starts from the beginning of the finned section and grows till the fully developed region. Also, figure (17) Shows that pressure starts with a high value at the inlet and decreases to zero-gauge pressure at the exit. Also, an important observation from the same figure is that the maximum pressure occurs at the fin face. This is because fins act like obstacles in the fluid stream. From figure (18), the thermal boundary layer begins developing from the start of heating and reaches the fully developed region at nearly 1 m from the inlet of the tube (0.5 meters from the heating start). Also, figure (18) reveals that the tip of any fin has a lower temperature, and this temperature increases along fin length due to the formation and growth of the boundary layer as mentioned earlier. Figure (19) shows velocity and temperature contours at 1 meter from the tube inlet. The figure reveals that the maximum velocity occurs at the core of the tube with the same distribution in the region between any two surfaces of the fins. Also, the figure depicts the formation of the boundary layer of the surfaces of both fins and tube and the merging of these boundary layers at the corner of the intersection of any fin root and the tube surface. The temperature contour temperature shows also the formation of a thermal boundary layer from the heating surface to the flow core which has the lowest temperature. Also, the figure shows that the temperature of the fin decreases along the fin height due to the loss of heat transfer through the fin surface. The symmetrical concept applied on temperature contour as applied on velocity one. These contours are drawn at mass flowrate equals 0.39188 kg/s and inlet temperature 25 ℃ and total heat of 5000 W.

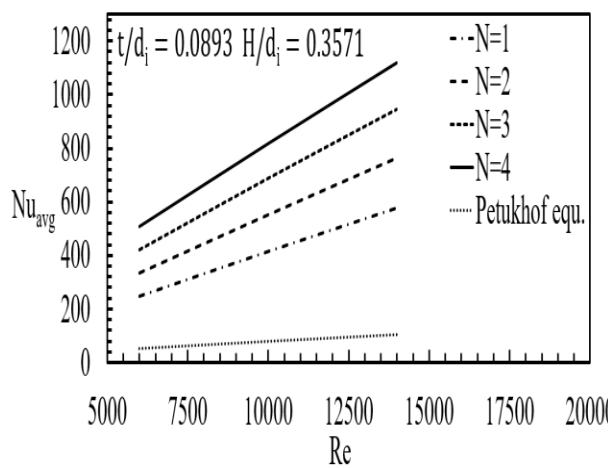


Figure (14)- Reynolds number effect on the average Nusselt number for the finned tube

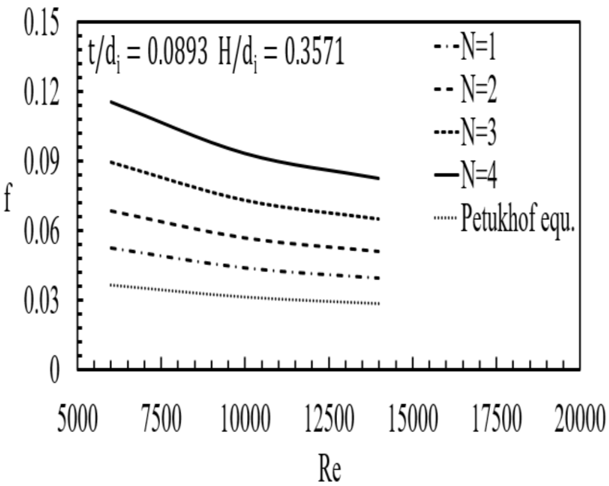


Figure (15)- Reynolds number effect on the average friction factor for the finned tube

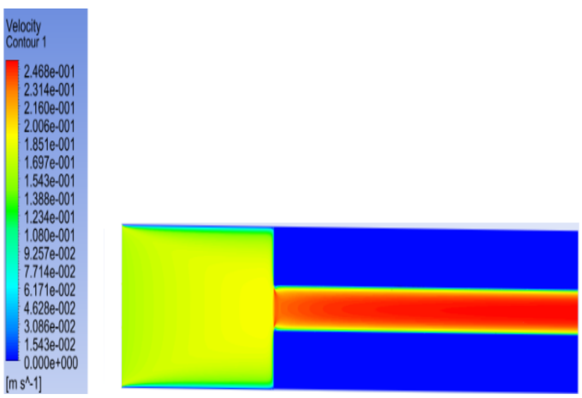


Figure (16)- Velocity contour at the tube center

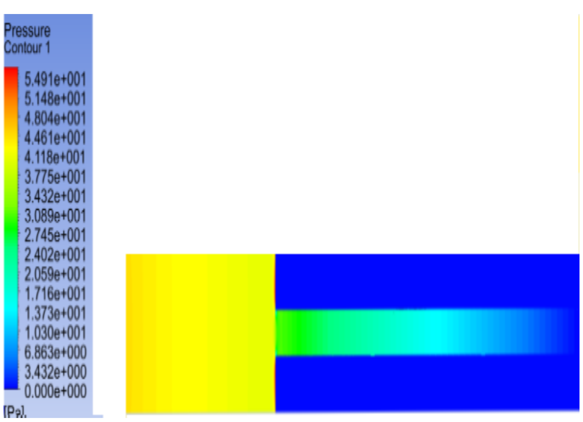


Figure (17)- Pressure contour at the tube center

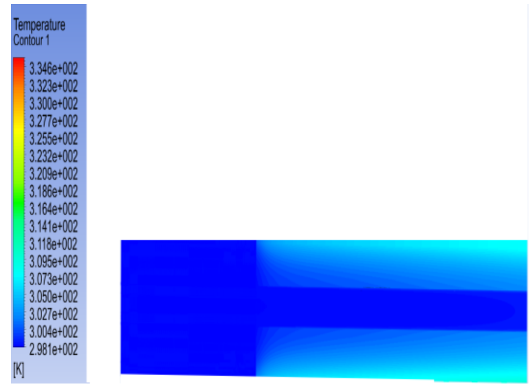


Figure (18)- Temperature contour at the tube center

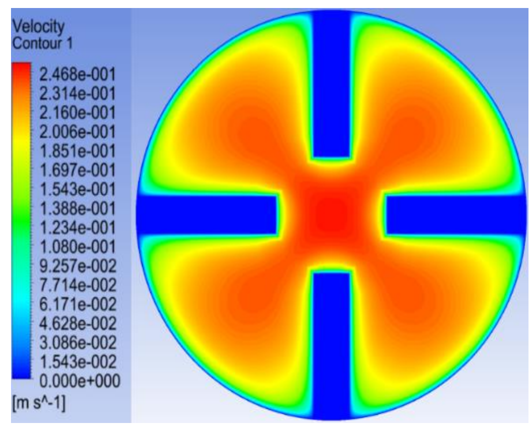


19.a. Velocity contour

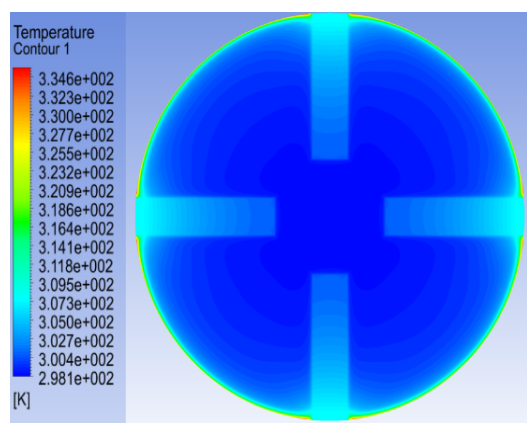


19.b. Temperature contour

Figure (19)- Cross-sectional contour at 1 m from the tube inlet

**8. Conclusions**

The conclusions of the present work can be summarized as follows:

1. It is found for the present work that the Nusselt number increases with the Reynolds number and the Prandtl number in both finless and finned tubes. In contrast, the friction factor decreases with the Reynolds number in both finless and finned tubes. Furthermore, it is found that the Prandtl number does not affect the friction factor.

2. From the present CFD results, at mass flowrate 0.39188 kg/s and fin height 20 mm, heat transfer coefficient rises by 97 % while the Nusselt number, which is based on hydraulic diameter, rises by 10 % as row number increases from 1 to 4. Also, the friction factor increases by 112.26 % while the friction factor, which based on hydraulic diameter, rises by 19.12 %.

3. From the present CFD results, at mass flowrate of 0.39188 kg/s and row number 4, the heat transfer coefficient rises by 194.6 % while the Nusselt number, which is based on hydraulic diameter, rises by 104.6 % as the fin height increases from 1 cm to 2 cm. Also, the friction factor increases by 86.17 % while the friction factor, based on hydraulic diameter, rises by 29.3%.

4. From the present CFD study, the results reveal that Nusselt number and friction factor increases by 7.8% and 8.6% respectively when the fin thickness increases from 2 mm to 6 mm. So fin width has no significant effect on the friction factor or the Nusselt number in finned tube. But, it is customary to use thick fins to be able to overcome erosion and corrosion, especially when using chemical reacting fluids in heat exchangers.

5. It can be also concluded from CFD results that fin height has a more significant effect on heat transfer enhancement than row number variation while fin height and fin number have nearly the same impact on friction factor. This is because of more turbulence generated due to fin height.

6. Generally, finned tube significantly enhances heat transfer compared to finless tubes.

7.

**9. Nomenclature**

| | |
|---|---|
| A | area |
| $C_p$ | specific heat |
| d | tube diameter |
| f | friction factor |
| H | fin height |
| h | heat transfer coefficient |
| I | turbulent intensity |
| K | turbulent kinetic energy |
| k | thermal conductivity |
| L | tube length |
| $\dot{m}$ | mass flowrate |
| N | number of rows |
| Nu | Nusselt number |
| Pr | Prandtl number |
| p | pressure |
| Q | total heat transfer |
| q | heat flux |
| Re | Reynolds number |
| S | strain |
| T | temperature |
| t | fin thickness |
| v | mean velocity |
| x | axial location |

**Greek symbols**

| | |
|---|---|
| $\alpha$ | thermal diffusivity |
| $\varepsilon$ | turbulent dissipation energy |
| $\mu$ | dynamic viscosity |
| $\upsilon$ | Kinematic viscosity |
| $\rho$ | density |
| $\tau$ | shear stress |

**Subscripts**

| | |
|---|---|
| avg | average |
| b | bulk |
| c | cross section |
| f | finned section |
| h | based on hydraulic diameter |
| i | inlet |
| m | mean |
| o | outlet |
| s | surface |
| t | turbulent |
| w | wall |
| x | local |

**10. References**

[1] M. Ahsan, "Numerical analysis of friction factor for a fully developed turbulent flow using k-ε turbulence model with enhanced wall treatment", Beni-Suef university journal of basic and applied sciences 3 (2014) 269-277.

[2] A. Bolukbasi, and B. Sahin, "Numerical investigation of turbulent forced convection flow in the horizontal tubes having constant heat flux", International Conference on Mechanical Engineering Research (ICMER2013), 1-3 July 2013.

[3] M. Everts, and J.P. Meyer, "Heat transfer of developing flow in the transitional flow regime", Proceedings of the 1st Thermal and Fluid Engineering Summer Conference, TFESC August 9-12, 2015.

[4] J.P. Meyer, M. Everts, N. Coetzee, K. Grote, and M. Steyn, "Heat transfer coefficients of laminar, transitional, quasi-turbulent and turbulent flow in circular tubes", International Communications in Heat and Mass Transfer 105 (2019) 84–106.

[5] A. Belhocine, and O. I. Abdullah, "Numerical simulation of thermally developing turbulent flow through a cylindrical tube", International Journal of Advanced Manufacturing Technology (2019) 102:2001–2012.

[6] A. Gbadebo, A. M. Said, and M. A. Habib, "Average Nusselt number correlation in the thermal entrance region of steady and pulsating turbulent pipe flows", Heat and Mass Transfer journal 35 (1999) 377-381.

[7] B. Sahin, E. Manay, and E. F. Akyurek, "An experimental study on heat transfer and pressure drop of CUO-water Nano fluid", Journal of Nanomaterials Volume 2015.

[8] M. Huq, and A. M. Aziz-UL Huq, "Experimental measurements of heat transfer in an internally finned tube", Int. Comm. Heat Mass Transfer, Vol. 25, No. 5, pp. 619-630, 1998.

[9] S. V. Patankar, M. Ivanovic, and E. M. Sparrow, "Analysis of Turbulent Flow and Heat Transfer in Internally Finned Tubes and Annuli", Journal of Heat Transfer, Feb. 1979, Vol 101.

[10] N. Kim, and R. L. Webb, "Analytic Prediction of the Friction and Heat Transfer for Turbulent Flow in Axial Internal Fin Tubes", Journal of Heat Transfer Aug. 1993, Vol. 115 / 553.

[11] T. C. Carnavos, "Cooling Air in Turbulent Flow with Internally Finned Tubes", heat transfer engineering vol.1 no.2 Oct.-Dec. 1979.

[12] T. C. Carnavos, "Heat Transfer Performance of Internally Finned Tubes in Turbulent Flow", heat transfer engineering vol.1 no.4 April - June 1980.

[13] M. D. Kailash, and M. Prasad, "Effect of fin and tube configuration on heat transfer of an internally finned tube", International Journal of Numerical Methods for Heat and Fluid Flow Vol.25 No.8, 2015.

[14] MD. A. Islam, and A. K. Mozumder, "Forced convection heat transfer performance of an internally finned tube", Journal of Mechanical Engineering, Vol. ME 40, No. 1, June 2009.

[15] K. Nandakumar, and J. H. Masliyah, "Fully developed viscous flow in internally finned tubes", Chemical Engineering Journal, 10 (1975) 113-l 20.

[16] H. M. Soliman, and A. Feingold, "Analysis of fully developed laminar flow in longitudinal internally finned tubes", The Chemical Engineering Journal, 14 (1977) 119 – 128.

[17] S. A. El-Sayed, S. A. El-Sayed, M. E. Abdel-Hamid, and M. M. Sadoun," Experimental Study of Turbulent Flow Inside a Circular Tube with Longitudinal Interrupted Fins in the Stream Wise Direction", Experimental Thermal and Fluid Science 1997, 15:1-15.

[18] S. A. El-Sayed, S. A. El-Sayed, and M. M. Sadoun, "Experimental Study of Heat Transfer to Flowing Air inside a Circular Tube with Longitudinal Continuous and Interrupted Fins", Journal of Electronics Cooling and Thermal control, 2012, 2, 1-16.

[19] G. Fabbrii, "Heat transfer optimization in internally finned tubes under laminar flow conditions", Int. J. Heat Mass Transfer.Vol.41. No.10, PP.1243-1253,1998.

[20] I. Alam, and P.S. Ghoshdastidar, "A study of heat transfer effectiveness of circular tubes with internal longitudinal fins having tapered lateral profiles", International Journal of Heat and Mass Transfer 45 (2002) 1371-1376.

[21] O. Zeitoun, and A. S. Hegazy, "Heat transfer for laminar flow in internally finned pipes with different fin heights and uniform wall temperature", Heat and Mass Transfer journal, 9 August 2003.

[22] D. Kim, "Thermal optimization of internally finned tube with variable fin thickness", Applied Thermal Engineering (2016).

[23] S. Kim, Kim, M. Kim, Y. G. Park, J. K. Min, and M. Y. Ha, "Numerical investigation of fluid flow and heat transfer characteristics in a helically-finned tube", Journal of Mechanical science and Technology 31 (7) (2017) 3271-3284.

[24] F. Khanmohammadi, M. Farhadi, A. A. Rabienataj, and R. Darzi, "Numerical investigation of heat transfer and fluid flow characteristics inside tube with internally star fins", Heat and Mass Transfer journal, August 2018.

[25] H.K. Versteeg, and W. Malalasekera," An introduction to computational fluid dynamics the finite volume method", 2nd edition.

[26] K. A. Yousef, A. S. Hegazy, and A. Engeda, "Use of vapor compression refrigeration system for cooling steam power plant condenser", full thesis, 2015.

[27] B.S. Petukhov, and V.N Popov," Theoretical calculation of heat exchange in turbulent flow in tubes of an incompressible fluid with variable physical properties", High Temp., (1/1): 69-83, 1963.